Supporting Information

3D imaging of gap plasmons in vertically coupled nanoparticles by EELS tomography

Georg Haberfehlner[1,2,*], Franz-Philipp Schmidt[2,3], Gernot Schaffernak[3], Anton Hörl[3], Andreas Trügler[3], Andreas Hohenau[3], Ferdinand Hofer[1,2], Joachim R. Krenn[3], Ulrich Hohenester[3], Gerald Kothleitner[1,2]

[1]Graz Centre for Electron Microscopy, Steyrergasse 17, 8010 Graz, Austria

[2]Institute of Electron Microscopy and Nanoanalysis, Graz University of Technology, Steyrergasse 17, 8010 Graz, Austria

[3]Institute of Physics, University of Graz, Universitätsplatz 5, 8010 Graz, Austria

[*]Corresponding author: georg.haberfehlner@felmi-zfe.at

S.1 Sample preparation

We prepared triangularly shaped silver/SiO_2/silver 3D dimers of 20/10/20 nm thickness by electron beam lithography (EBL) in a RAITH eLINE Plus system using a poly(methylmetacrylate) (PMMA) resist on a 5 nm thick silicon nitride (Si_3N_4) membrane (for both optical and EELS measurements) and a standard silver evaporation and lift-off procedure.[1] The side length of the equilateral triangle ranged between approximately 140 to 340 nm. All layers were evaporated into the same PMMA mask for optimized vertical stack alignment. A lateral shrinkage of the upper silver triangle from 11% (for the largest triangle) to 18% (for the smallest triangle) with respect to the lower triangle was observed due to material deposition on the edges of the mask opening that reduces its size during the deposition process. Before the EELS measurements the samples were coated with a thin layer (1-2 nm) of carbon, to prevent charging of the nanostructures.

S.2 Optical measurements

The optical measurements were performed on particle arrays, arranged non-periodically to avoid the occurrence of grating effects. The triangles had defined orientation, but random position, with a minimum interparticle distance of 1.5 times the particle size ensuring that no near field interaction of the individual particles takes place. The measurement was done with a 10x objective, numerical aperture = 0,075 over an area of $(20\ \mu m)^2\pi$, averaging over 2000 to 9000 particles, depending on the size of the individual 3D dimers.

To retrieve the extinction of the structures, the optical transmission of the particle array was measured for wavelengths in the range of 390-1100 nm. The transmission of the Si_3N_4 membrane was used as reference signal. The measurement was performed for two orthogonal polarization directions, yielding

virtually identical results, as the equilateral triangle has its dipole resonances at the same energy for both polarization directions oriented along triangle side and triangle height.

S.3 EELS acquisition

The EELS experiments were performed on a probe-corrected FEI Titan[3] 60-300 microscope operated at 300 kV, with an X-FEG field-emission electron gun and a Wien-type monochromator operated in decelerated gun lens mode, with the excitation set to a value of 0.8. The energy spread of the monochromated beam was measured to be 170 meV (full-width at half-maximum of the zero-loss peak). The beam convergence semi-angle was 15 mrad, the collection semi-angle was 20.5 mrad. EELS spectra were acquired on a Gatan Imaging Filter (GIF) Quantum with 5x vertical binning. All spectrum images were acquired with sizes in the range of 130*130 pixels with exposure time of 0.5 ms per pixel. For the acquisition of the tilt series of T1 the pixel size was 1.9 nm, for T2 the pixel size was 2.9 nm. The tilt series of EELS spectrum images for T1 and T2 were acquired over a range of about +/-75° with tilt steps of 5°.

S.4 EELS data processing

Spectrum images were aligned in energy based on the position of the zero-loss peak and binned by a factor of two in the two spatial dimensions (reducing the sizes of the spectrum images to 65*65 pixels). Subsequently, the spectra were normalized by the zero-loss peak intensity and deconvolved with a Richardson-Lucy deconvolution with 25 iterations with an analysis program for spectrum images "SI analysis tool".[2] Spectra in two corners of the binned spectrum image, away from the sample structure, were averaged over 2*15*15 pixels and used as point-spread function for deconvolution. To extract 2D maps of surface plasmon resonances, the spectra were integrated over an energy region of 0.2 eV around the peak in the deconvolved spectrum images.

As the samples were stored for about a week between acquisition of the 2D spectrum images and the tomographic series ageing was observed, with the likely formation of oxide or sulfide on the surface of the sample and structural changes of silver.[3] This led to a red-shift of about 0.2 eV and damping of the dipolar modes for samples of the same size before and after ageing. However, the two dipolar modes are still clearly identifiable in the aged samples (see Fig. S4). During acquisition of the tilt series, contamination slowly built up on the sample. This led to a further red-shift of 0.1 eV which can be identified when comparing spectra acquired before, during and after the tilt series (see Supporting Fig. 4). The extracted maps remain similar even with the build-up of contamination, classifying them for tomographic reconstruction. We compensated for this red-shift during the tilt series by shifting the integration windows. For this purpose we identified the resonance energy of each peak in spectrum images recorded just before and just after acquisition of the tilt series. These two values were used as starting and end point for the peak position. For each spectrum image acquired during the tilt series the peak position for the extraction of 2D maps was shifted by a constant step in energy.

S.5 Tomographic alignment

Alignment of the tomographic tilt series was done based on the HAADF STEM images acquired at the same time as the EELS spectrum images. To remove the influence of the background signal on the alignment, first of all the absolute minimum of each projection was subtracted from every pixel in the projection. Afterwards, a mask was created using thresholding and morphological operations to select only pixels in which the triangles are projected. All pixels outside of this mask are set to zero. These masked projections were used for the alignment with center of mass methods.[3,4] The calculated alignment parameters were applied to align both the HAADF STEM tilt series and the tilt series of EELS spectrum images.

S.6 Reconstruction of the HAADF STEM tilt series

The simultaneously acquired HAADF STEM tilt series was reconstructed using a total-variation (TV) minimization algorithm using a full 3D algorithm as described in previous work.[5] In TV minimization it is assumed that the volume gradient is sparse, i.e. is zero at most locations. This leads to sharp interfaces between different regions. A 3D adaptation of the TV minimization solver TVAL3[6] was used in combination with GPU-based projection and reprojection operators from the ASTRA toolbox.[7] The reconstruction was segmented using an absolute threshold value to define the dimers. From the segmented volume a triangulated surface was calculated, which served as input for the simulation and reconstruction of the plasmon fields. The number of triangulation elements was 1000 for the dimer T1 and 1700 for T2.

S.7 Simulations

The optical and EELS simulations for the two geometries were carried out with the MNPBEM-Toolbox[8,9] and we used a silver dielectric function extracted from optical experiments[10]. For simulations of EELS spectra, the surface reconstruction obtained from HAADF STEM tomography was used for both optical and EELS simulations. To observe the effect of coupling on the dipole resonances, EELS simulations were also done for individual triangles. The substrate and intermediary oxide layer were not taken into account, but simulations were done with either a refractive index of n = 1 or 1.4 for the medium surrounding the particles to mimic environment effects.

EELS spectra were simulated for a 2D grid of beam positions similar to the experimental spectrum image acquisition. For comparison to the experiment, the spectra for all beam positions were summed up. For the EELS maps, the simulated spectra for each beam position were summed over an energy region of 0.2 eV around the peak position. EELS simulations were carried out with the beam direction perpendicular to the particle surface (usual geometry for EELS experiments).

S.8 Reconstruction of surface plasmon maps

The reconstruction of the photonic LDOS was performed as described in Ref.[11]. Based on reconstructions of the nanoparticle surface, the plasmonic eigenmodes $\boldsymbol{E_k}(r)$[12] were calculated by computing the eigenvalues and eigenvectors of the matrix from a boundary element approach (see Eq. 21 of Ref. [13]), at the frequencies of the plasmon resonances extracted from the simulated EELS spectra. These served as a generic basis for the decomposition of the Green tensor

$$\boldsymbol{G}(\boldsymbol{r},\boldsymbol{r'}) \approx \sum_{k=1}^{n} C_k \boldsymbol{E_k}(\boldsymbol{r}) \otimes \boldsymbol{E_k}(\boldsymbol{r'}) \qquad \text{(S1)}$$

which provides a complete characterization of the photonic environment of the plasmonic nanoparticle for given expansion coefficients C_k.

The coefficients C_k were determined by solving the L1/L2 optimization

$$\min_{C_k} \left[\|C_k\|_1 + \frac{1}{2\mu} \left\| P_{exp} - P_{rep} \right\|_2^2 \right] \qquad \text{(S2)}$$

In this optimization the second term minimizes the difference between measured EELS data $P_{exp}(\boldsymbol{R},\theta)$ and reprojected EELS data $P_{rep}(\boldsymbol{R},\theta)$, which can be calculated for a set of coefficients C_k using the standard EELS equations.[14] The first term enforces sparsity on the coefficient vector C_k, i.e. it leads to a Green function decomposition with as few nonzero expansion coefficients as possible. The compressed sensing minimization was performed with the toolbox YALL1 (online at http://yall1.blogs.rice.edu). The mixing parameter was set to μ = 0.5, leading to a good agreement between measured and reprojected data, while still strongly restricting the number of nonzero coefficients in the eigenmode basis.

In the optimization, we used 10000 random data points from the EELS measurement outside the particles and at least 5 nm away from the particle boundary. Data inside the particle were not used as they are quite noisy due to the relatively high thickness of the two (tilted) silver layers. Reprojections of EELS maps are compared with EELS measurements in Fig. S4.

References

(1) Hohenau, A.; Ditlbacher, H.; Lamprecht, B.; Krenn, J. R.; Leitner, A.; Aussenegg, F. R. *Microelectron. Eng.* **2006**, *83*, 1464–1467.
(2) Schmidt, F. P.; Hofer, F.; Krenn, J. R. *Micron* **2017**, *93*, 43–51.
(3) Haberfehlner, G.; Trügler, A.; Schmidt, F. P.; Hörl, A.; Hofer, F.; Hohenester, U.; Kothleitner, G. *Nano Lett.* **2015**, *15*, 7726–7730.
(4) Azevedo, S. G.; Schneberk, D. J.; Fitch, J.; Martz, H. E. *IEEE Trans. Nucl. Sci.* **1990**, *37*, 1525–1540.
(5) Haberfehlner, G.; Orthacker, A.; Albu, M.; Li, J.; Kothleitner, G. *Nanoscale* **2014**, *6*, 14563–14569.
(6) Li, C.; Yin, W.; Jiang, H.; Zhang, Y. *Comput. Optim. Appl.* **2013**, *56*, 507–530.
(7) Palenstijn, W. J.; Batenburg, K. J.; Sijbers, J. *J. Struct. Biol.* **2011**, *176*, 250–253.
(8) Hohenester, U.; Trügler, A. *Comput. Phys. Commun.* **2012**, *183*, 370–381.
(9) Hohenester, U. *Comput. Phys. Commun.* **2014**, *185*, 1177–1187.
(10) Johnson, P. B.; Christy, R. W. *Phys. Rev. B* **1972**, *6*, 4370–4379.
(11) Hörl, A.; Trügler, A.; Hohenester, U. *ACS Photonics* **2015**, *2*, 1429–1435.

(12) Sauvan, C.; Hugonin, J. P.; Maksymov, I. S.; Lalanne, P. *Phys. Rev. Lett.* **2013**, *110*, 237401.
(13) García de Abajo, F. J.; Howie, A. *Phys. Rev. B* **2002**, *65*, 115418.
(14) García de Abajo, F. J. *Rev. Mod. Phys.* **2010**, *82*, 209–275.
(15) Schmidt, F. P.; Ditlbacher, H.; Hofer, F.; Krenn, J. R.; Hohenester, U. *Nano Lett.* **2014**, *14*, 4810–4815.

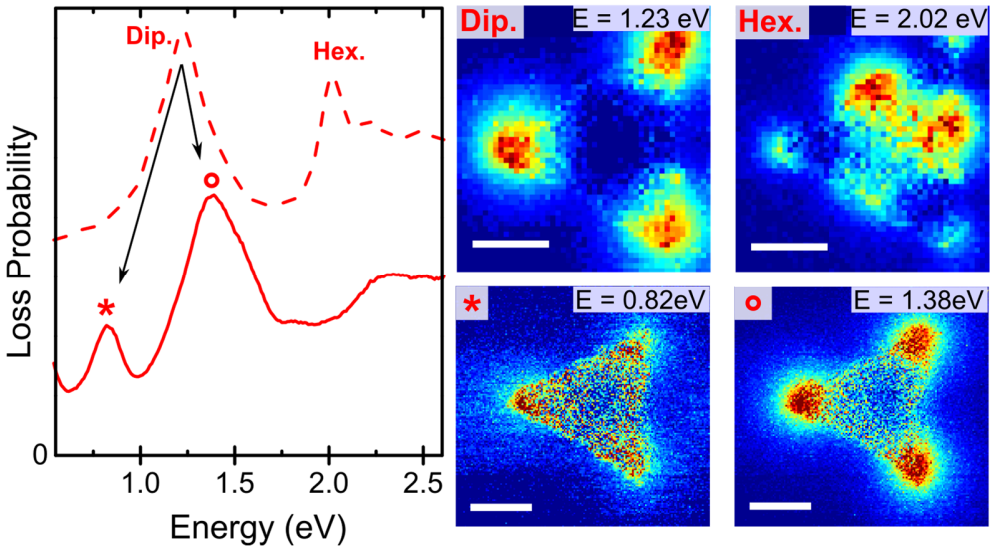

Figure S1. Splitting of the dipole mode. The dashed line (top) spectrum is summed over a spectrum image taken from a single triangle on a Si_3N_4 substrate, showing a dipolar (Dip.) and hexapolar (Hex.) peak, which can be identified in the EELS maps (top right row).[15] No peaks are visible at energies below the dipolar peak or between the dipole and hexapole peaks. The solid line (bottom) spectrum is summed over a spectrum image taken from a stacked dimer. Here, two dipole resonances are visible. The dashed line is shifted by a constant offset. Scale bars are 100 nm.

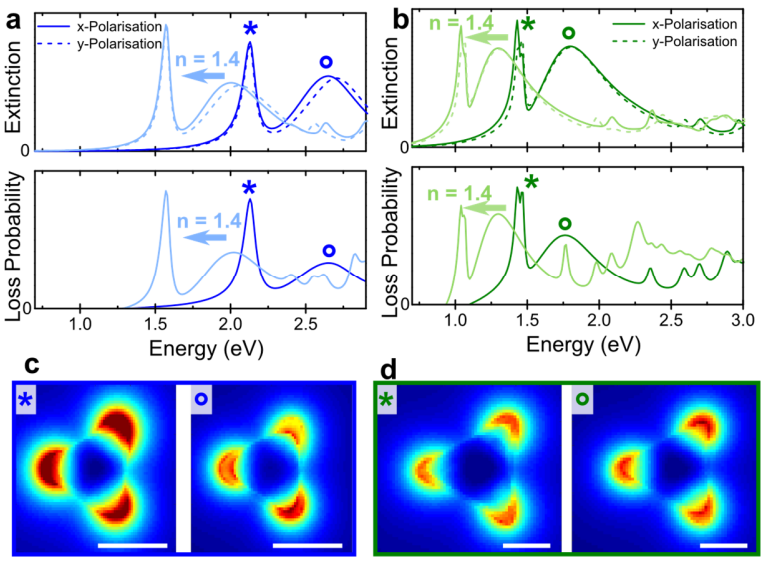

Figure S2. Numerical simulations based on the reconstructed particle morphology. Optical extinction spectra (top) and EELS spectra (bottom) of (a) T1 and (b) T2. The dark (blue and green) lines are calculated without including the substrate and the insulating layer between the silver particles, i.e., assigning a refractive index of 1 to both of them. For the spectra drawn in light colors the refractive index of the surrounding medium and of the insulating layer was set to n = 1.4 (close to the refractive index of SiO_2 and smaller than the refractive index of Si_3N_4 and carbon), showing that an higher index environment leads to a red shift of resonance peaks. The optical spectra are simulated for two perpendicular polarizations (shown in solid and dashed lines). The asymmetry of the particle geometry, leads to small differences between the polarizations for the lower energy mode and to a twin peak in the EELS simulated EELS spectrum. Spectral features at higher energies stem from multipole, breathing and interface modes. (c), (d) Simulated EELS maps extracted for the two resonance energies indicated in the spectrum for (c) T1 and (d) T2. Scale bars are 100 nm.

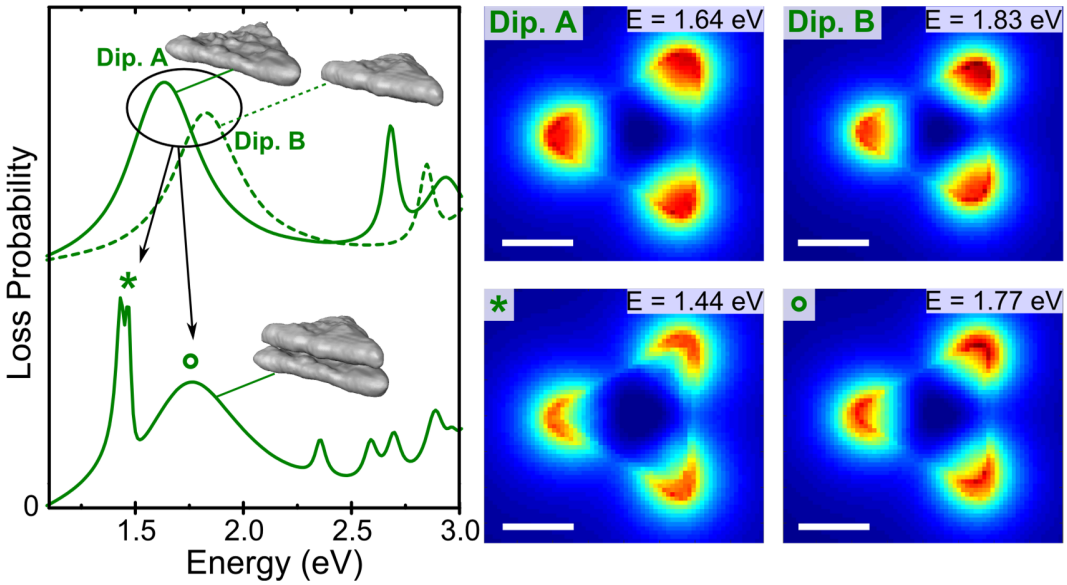

Figure S3. Simulation of single triangles and a dimer based on the reconstructed morphology of T2. The top spectra show simulations of single triangles, using the morphology of the two individual (top and bottom) reconstructed triangles. For each simulation a single dipole peak appears. The solid line is a simulation of the lower triangle of the dimer, which shows a dipole peak (Dip. A) at 1.64 eV, the dashed line refers to the upper triangle, showing a dipole peak (Dip. B) at a slightly higher energy (1.83 eV). In the bottom spectrum the full dimer is simulated, where the dipole mode splits into two peaks (* and °), which change in shape and are shifted with respect to the modes on the individual triangles. The simulated EELS maps at the indicated energies are depicted on the right hand side. Spectra of individual triangles are shifted by a constant offset. Scale bars are 100 nm.

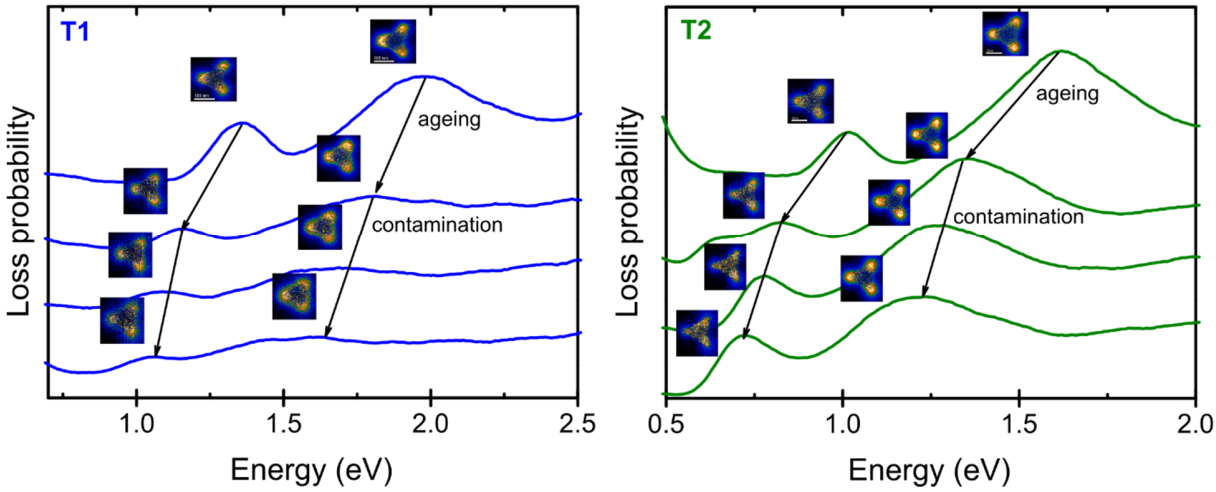

Figure S4. Effects of ageing and contamination on the dipole resonances. The black lines show spectra acquired on a fresh sample. The red lines were recorded at the beginning of the tilt series, after the sample was stored for a few days, showing peak shifts due a change of the optical properties of silver over time. The green lines were recorded during and the blue lines after the tilt series, showing contamination-induced peak shifts.